Efficiency of pump absorption in double-clad fiber amplifiers. I. Fiber with circular symmetry

Dmitrii Kouznetsov and Jerome V. Moloney

Arizona Center for Mathematical Sciences, Department of Mathematics, University of Arizona, 617 North Santa Rita, Tucson, Arizona 85721

Ewan M. Wright

Optical Sciences Center, University of Arizona, Tucson, Arizona 85721

Received May 16, 2000; revised manuscript received February 16, 2000

The paraxial propagation of spatially random monochromatic light in a fiber with an absorbing core is treated as a model for pump absorption in a double-clad optical fiber amplifier. Mode coupling caused by fluctuations of the index of refraction is considered a mechanism that increases the pump absorption and is analyzed in the speckle-mode approximation for the example of a Kerr nonlinearity. The original method of approximate images is described; it allows the use of a fast Fourier transform for numerical simulations in curvilinear regions. Simulations demonstrate the validity of the speckle-mode estimations. For a continuous-wave pump in silica fibers, the electronic Kerr effect is shown to be too small to enhance pump absorption; however, estimates show that the thermal nonlinearity may have a significant effect. The electronic Kerr nonlinearity in the cladding can be significant for a pulsed pump source.

OCIS codes: 140.3510, 190.4370, 060.2320.

1. INTRODUCTION

Double-clad fiber amplifiers provide an effective way to transfer the energy of partially coherent light from semiconductor lasers into single-mode radiation.[1–3] In the simplest geometry the pump propagates in a broad-core optical fiber, which plays the role of a cladding for the narrow amplifying core. The maximal output power of a single-mode double-clad fiber laser is limited by the power of the pump and the efficiency of the coupling of the pump into the core[3–6]; a geometrical optics approximation allows the estimation of the efficiency of absorption of the pump in the core for various cases. In this paper we present the results of a wave-optical approach to the same problem for the case of a circular fiber with a nonlinear cladding. Also, we develop an original method of approximate images, which allows generalization to the case of noncircular fibers.

Fluctuations of the refractive index in a double-clad fiber can provide significant mixing of the modes of the unperturbed fiber. Since most of the unperturbed modes almost do not overlap the absorbing core, the mode mixing can significantly increase the pump absorption. We estimate that, for realistic fibers, spatially varying fluctuations $\delta n/n$ of the order of 10^{-4} may provide such a mixing. Such small fluctuations may have many origins, and they are difficult to measure experimentally. As a specific illustration we consider self-phase modulation caused by the Kerr nonlinearity, which could be either electronic or thermal in origin. There are reasons in favor of such a choice. The efficiency of the pump in unperturbed cylindrical fibers is low.[5,6] Thus any mechanism of modes mixing should be clearly seen in experiments, as well as in the simulations. The Kerr constant is known; so, for a given field, we can explicitly calculate the index of refraction. For a pulsed pump and a highly homogeneous cladding, the fluctuations induced by the Kerr nonlinearity should dominate. This should allow an easy experimental test of our results. Note that the power of the pump is the easiest parameter to vary during experiments. The dependence of the efficiency on this parameter can be measured without modifying of the experimental setup.

We analyze the role of inhomogeneities in the cladding, considering the Kerr nonlinearity as a possible way to improve the coupling of the modes of the cladding into the core. We expect our results to be useful for estimation of the role of any other inhomogeneities in the cladding. At least a qualitative estimate of the role of such fluctuations can be performed on the basis of our results for the Kerr nonlinearity. In addition, we expect that our method of simulation will be useful not only for fibers with circular symmetry but also for any other convex cladding.

We make an asymptotic estimation based on the geometrical optics and the speckle-mode approximation. This estimate leads to a system of two ordinary differential equations for the power in the coupled and the uncoupled modes. On the basis of these equations, we analyze the significance of fluctuations of the index of refraction in realistic fibers. We describe the original method of approximate images for conducting numerical simulations. We apply this method to test our analytical results. Finally, we estimate the role of thermal nonlinearity in the mixing of modes.

0740-3224/2001/060743-07$15.00

2. COUPLED AND UNCOUPLED MODES

In this section we write the basic equations and analyze the efficiency of the pumping of the core in terms of geometrical optics.

If we neglect the core, then the paraxial propagation of the quasi-monochromatic field $\mathrm{Re}[E(\mathbf{x}, z)\exp(ikz - i\omega t)]$ can be described with the equation

$$\frac{\partial E}{\partial z} = \frac{i\Delta_\perp}{2k} E,$$

where $\mathbf{x} = \{x_1, x_2\}$, $k = 2\pi/\lambda$ is the wave number in the cladding, and $\Delta_\perp = \partial^2/\partial x_1^2 + \partial^2/\partial x_2^2$. Assume that the field practically disappears outside of the cladding. This gives the boundary condition $E(\mathbf{x}, z) = 0$ at $|\mathbf{x}|^2 = R^2$, where R is the radius of the cladding (see Fig. 1).

The solution of the paraxial equation can be written as an expansion in Bessel modes Ψ:

$$E(\rho\cos\phi, \rho\sin\phi, z) = \sum_{m=-\infty}^{\infty} \sum_{j=1}^{\infty} C_{m,j}\Psi_{m,j},$$

$$\Psi_{m,j} = \mathrm{J}_m(q_{m,j}\rho/R)\exp[im\phi - i(q_{j,m}/R)^2 z/(2k)], \quad (1)$$

where J_m is the Bessel function of the mth order, $q_{m,j}$ is the jth solution of the equation $\mathrm{J}_m(q) = 0$, and C denotes arbitrary complex coefficients.

The core can be taken into account by addition of the term $-ik\nu E$ on the right-hand side of the paraxial equation, where $\nu = \nu(|x|)$ is the relative variation of the complex index of refraction; its imaginary part describes absorption. This dependence on spatial coordinates can be approximated with a step function, $\nu(\rho) = \nu_0 = (n_{\mathrm{core}} - n_{\mathrm{clad}})/n_{\mathrm{clad}}$ at $\rho < r$, and $\nu(\rho) = 0$ at $\rho > r$, where r is radius of the core (Fig. 1).

Functions (1) give the natural basis for the expansion of the field in fibers with circular cladding. Nevertheless, for the simulation below we use another method (the method of approximate images) that seems to be flexible with respect to changes of cladding geometry, and we plan to investigate this characteristic as a continuation of this research.

Formally, all modes ψ are coupled to the core of any positive radius r; but, as the angular mode number m increases, the coupling decreases as $(r/R)^{|m|}$ and soon becomes very small. How can one estimate the percentage of effectively coupled modes? To do this we use the following assumption based on geometrical optics[5]: The number of coupled modes is proportional to the number of coupled rays. Then, instead of modes, we consider the ensemble of rays with various helicities passing through each point $\{\rho\cos\phi, \rho\sin\phi\}$ of the cladding cross section.

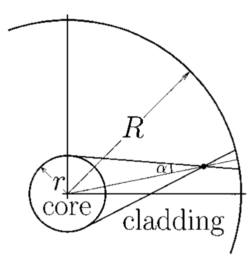

Fig. 1. Cross section of the symmetrical double-clad fiber.

Note that if the ray crosses the core once it will cross it at every trip between reflections from the wall of the cladding, owing to the symmetry. The probability P_ρ that the ray crosses the core $P_\rho = 2\alpha/\pi$ is the simple ratio of the quadrupled angle $\alpha = \arcsin(r/\rho)$ to the whole angle 2π. Taking the mean value (average) of P_ρ with respect to the cross section of the cladding, we get an estimate of the percentage of coupled rays:

$$\eta = \frac{\int_r^R P_\rho \rho \mathrm{d}\rho}{\int_r^R \rho \mathrm{d}\rho} \approx \frac{4r}{\pi R}. \quad (2)$$

To get this approximation, we assumed that $r/R \ll 1$. This formula can also be obtained as the limit case of formula (7) of Ref. 5.

The asymptotic formula (2) allows comparison with an experiment. Reference 6 reports experimental results for the symmetric fiber with $r = 3.3\ \mu\mathrm{m}$, $R = 160\ \mu\mathrm{m}$. For three different wavelengths Bedö *et al.*[6] present a value of P_n', which is equivalent to our $1 - \eta$. The mean value of their data gives the value $P_n' = 0.9713$, which agrees with value $1 - \eta = 0.9737$ evaluated with formula (2).

The mean absorption rate κ of any coupled ray depends on its minimal distance h from the optical axis:

$$\kappa(h) = 2k\,\mathrm{Im}(\nu_0)\sqrt{r^2 - h^2}/R.$$

Consider the mean value over all possible rays:

$$\kappa = \frac{1}{r}\int_0^r \kappa(h)\mathrm{d}h = \frac{\pi^2}{8}\eta k\,\mathrm{Im}(\nu_0). \quad (3)$$

If we neglect the difference between various coupled modes, the evolution of the total power A of all coupled modes in the absence of nonlinearity can be described with the equation $\mathrm{d}A/\mathrm{d}z = -\kappa A$. This gives us $A(z) = A(0)\exp(-\kappa z)$.

Let B be the power of all uncoupled modes. Then the total power in the cladding $W(z) = B + A = B(0) + A(0)\exp(-\kappa z)$. Let $W_0 = A(0) + B(0)$ be the initial power of the pump. Then $A(0) = \eta W_0$, $B(0) = (1 - \eta)W_0$, and we get the estimate of the efficiency of core pumping as a ratio of the absorbed power to the initial power: $\mathcal{D} = (W_0 - A - B)/W_0 = \eta[1 - \exp(-\kappa z)]$. In this approximation the efficiency $\mathcal{D}$ depends neither on the real part of ν_0 nor on the scale of the transverse modulation of the pump.

3. INTRAMODULATIONAL NOISE

To take into account the possible nonlinearity of the cladding, consider the equation

$$\frac{\partial E}{\partial z} = \frac{i\Delta_\perp}{2k}E + ik\nu E + i\gamma|E|^2 E, \quad (4)$$

where $\gamma = (n_2/n_{\mathrm{clad}})k$. For the case of complete modulation and a small mean intensity, and for a very large cladding and a very small core, we may consider the nonlinear effect as in a bulk medium. Then within the speckle-mode approximation[7–9] we write the propagating field as $E = E_0 \exp(2i\gamma wz) + J$, where E_0 is the solution of Eq. (4) at $\gamma = 0$, $w = \langle EE^* \rangle$ is the average value of the intensity over the cross section, and J is some intramodulational noise. The mean noise intensity increases as $\langle JJ^* \rangle \approx 2\gamma^2 w^3 L_{\mathrm{dif}} z$, where L_{dif} is the diffraction length of the field. The coefficient $2\gamma^2 w^3 L_{\mathrm{dif}}$ should be interpreted as the rate of intermodal exchange. Then the rate of redistribution of power is given by $g = 2L_{\mathrm{dif}}\gamma^2 w^3 \pi R^2 = 2L_{\mathrm{dif}}[\gamma W/(\pi R^2)]^2 W$, where $W = \pi R^2 w$ is the total power in all modes.

Let a be the mean intensity among coupled modes and b be the mean intensity among the uncoupled ones. Let N be the total amount of excited modes in the cladding. Then assume that $1/N$ part of this power goes to each of the modes, whether they are coupled or uncoupled. (This assumption implies a quasi-isotropic structure of field modulation over most of the cross section of the inner cladding.) Also, each mode of intensity a loses its intensity at the rate ga/W, and each mode of intensity b loses its intensity at the rate gb/W, just owing to the intermodal exchange. This mechanism makes no distinction between coupled and uncoupled modes. The absorption deals with only the coupled modes, making them lose their mean intensity with the additional decrement κ. So we write the equations of the balance of intensities of coupled and uncoupled modes:

$$\frac{\mathrm{d}a}{\mathrm{d}z} = -\kappa a + g\frac{1}{N} - \frac{ga}{W},$$

$$\frac{\mathrm{d}b}{\mathrm{d}z} = g\frac{1}{N} - \frac{gb}{W}.$$

Multiplying the first equation by the factor ηN and the second one by $(1 - \eta)N$ and using the notation A and B of the previous section, we write the total intensity of coupled modes as $A = N\eta a$ and the total intensity of uncoupled modes as $B = N(1 - \eta)b$. Taking into account that $W = A + B$, we get

$$\frac{\mathrm{d}A}{\mathrm{d}z} = -\kappa A + 2L_{\mathrm{dif}}\left[\frac{\gamma(A + B)}{\pi R^2}\right]^2 [\eta B - (1 - \eta)A], \quad (5)$$

$$\frac{\mathrm{d}B}{\mathrm{d}z} = -2L_{\mathrm{dif}}\left[\frac{\gamma(A + B)}{\pi R^2}\right]^2 [\eta B - (1 - \eta)A]. \quad (6)$$

Let p_0 be the maximal transverse wave number presented in the expansion of the field with respect to plane waves. This parameter can be estimated as the product of the wave number k and the numerical aperture of the incident beam. (We assume $p_0 \ll k$.) Then we can estimate the diffraction length L_{dif}, assuming that, after propagation of a diffraction length in free space, the highest Fourier components change their phase so that the real part of their projection to the initial field becomes zero: $\mathrm{Re}[\exp(-ip_0^2/(2k)L_{\mathrm{dif}})] = 0$. This gives an estimate for the diffraction length: $L_{\mathrm{dif}} = \pi k/p_0^2$. Using this estimate, we introduce the constant of intermodal exchange

$$G = 2\pi\left(\frac{\gamma}{\pi R^2}\right)^2 \frac{k}{p_0^2} \quad (7)$$

and express the evolution of the power of coupled and uncoupled modes as follows:

$$\mathrm{d}A/\mathrm{d}z = -\kappa A + G(A + B)^2[\eta B - (1 - \eta)A], \quad (8)$$

$$\mathrm{d}B/\mathrm{d}z = -G(A + B)^2[\eta B - (1 - \eta)A]. \quad (9)$$

One can confirm that the system of Eqs. (7)–(9) is invariant with respect to the dilatation transformation

$$r \to Mr, \qquad R \to MR, \qquad p_0 \to M^{-1}p_0,$$

$$z \to M^2 z, \qquad \nu \to M^{-2}\nu, \qquad E \to M^{-1}E, \quad (10)$$

where the dimensionless parameter M of dilatation should not be too small, to satisfy the condition $p_0 \ll k$.

In the case of weak nonlinearity and a small core ($\eta B^2 G \ll \kappa$), we may neglect terms with A in Eq. (9); then $\mathrm{d}B/\mathrm{d}z = -\eta G B^3$. While $B(0) \approx W_0$, we can write

$$B = B(z) \approx \frac{W_0}{(1 + 2\kappa_{\mathrm{eff}} z)^{1/2}}, \quad (11)$$

where

$$\kappa_{\mathrm{eff}} = \frac{\pi k\,\eta}{2p_0^2}\left(\frac{2\gamma W_0}{\pi R^2}\right)^2. \quad (12)$$

We see that κ_{eff} should be interpreted as the effective nonlinear absorption rate. Define the following effective parameters:

(A) The nonlinear correction of the wave number: $Q = 2\gamma W_0/(\pi R^2) = 2\gamma w_0 = 2(n_2/n_{\mathrm{clad}})w_0$,

(B) The mean variation of the effective index of refraction: $\delta n = 2n_2 W_0/(n_{\mathrm{clad}}\pi R^2)$,

(C) The self-focusing power $W_{\mathrm{sf}} = n_{\mathrm{clad}}/n_2 k^2$.

Now we express the the effective absorption rate as

$$\kappa_{\mathrm{eff}} = \frac{2rk}{Rp_0^2}Q^2, \quad (13)$$

$$\kappa_{\mathrm{eff}} = \frac{8rk^3}{Rp_0^2}(\delta n)^2, \quad (14)$$

$$\kappa_{\mathrm{eff}} = \frac{8r}{\pi^2 R^5 k p_0^2}\left(\frac{W_0}{W_{\mathrm{sf}}}\right)^2. \quad (15)$$

The length of propagation L at which such nonlinear mixing becomes effective can be expressed as $1/\kappa_{\mathrm{eff}}$.

We now estimate the orders of magnitude of the pump power, for which the electronic Kerr nonlinearity may become significant. A typical value of the constant n_2 is $2.6 \times 10^{-16}\,\mathrm{cm^2/W}$ for silica glasses.[10] The peak pump power $W = 10^7\,\mathrm{W}$ is quite attainable, at least for short pulses. Then, at $r = 10^{-3}\,\mathrm{cm}$, $R = 10^{-2}\,\mathrm{cm}$, $k = 10^5\,\mathrm{cm^{-1}}$, and $p_0 = 0.1k$, we have $\delta n \approx 10^{-4}$ and $\kappa_{\mathrm{eff}} \approx 0.001\,\mathrm{cm^{-1}}$, which yields $1/\kappa_{\mathrm{eff}} \approx 10\,\mathrm{m}$. The estimate above shows that nonlinear mode mixing is realizable for short-pulsed pumps.

It should be noted, however, that in most practical applications of double-clad fibers one uses a continuous pump. The continuous source of power used in the estimate above is not attainable. This indicates that the nonlinear mode mixing that is due to the electronic Kerr effect is not relevant with a continuous pump in silica fibers.

Nevertheless, the estimate above does not at all eliminate the possibility of observing nonlinear mode mixing in fiber amplifiers with a continuous pump. We note that for polymer optical fibers[11–13] values of the nonlinear constant $n_2 \approx 4 \times 10^{-12}\,\mathrm{cm}^2/\mathrm{W}$ have been reported, which are 4 orders of magnitude greater than for silica fibers. Colored fibers[14,15] could give an even stronger effect. Also, we expect that the thermal nonlinearity is much stronger than the Kerr nonlinearity. We discuss the relevance of the thermal Kerr nonlinearity in Section 5.

From the estimate above we conclude that fluctuations of the index of refraction of the order of 10^{-4} may cause significant mode mixing independently of the origin of such fluctuations. For example, internal inhomogeneities with appropriate correlational properties could significantly improve the coupling of pump power into the core. Thus we expect that experimental efforts to improve the homogeneity of the refractive index of the cladding of the fiber amplifier may cause a reduction of the efficiency instead of an improvement.

4. WAVE-OPTICAL SIMULATIONS

The asymptotic approximation of the previous sections takes into account only two groups of modes, coupled and uncoupled, making no distinction between various coupled modes. Here we solve Eq. (4) numerically and compare the results with solutions of Eqs. (8) and (9).

To reduce discretization errors, we approximate the variation of the refractive index with a smooth function $\nu(\rho\cos\phi, \rho\sin\phi) = \nu_0(1 - \exp[-(\rho/r)^l])$. The value $l = 20$ was used, and we see almost no differences in the values of $\mathcal{D}$ evaluated from the simulations with l doubled.

To construct a class of initial conditions $E(\mathbf{x}, 0)$, we begin with δ-correlated Gaussian noise $E_{\mathbf{p}}$; all components are independent at this stage. Then, we treat $E_{\mathbf{p}}$ as Fourier components of the field and truncate by setting them to zero at $|\mathbf{p}| > p_0$. Such a truncation can be described with projector $\mathcal{T}$: $\mathcal{T}E_{\mathbf{p}} = E_{\mathbf{p}}\theta(p_0 - |\mathbf{p}|)$. Then the field can be calculated as the inverse transform of the truncated noise.

To satisfy the boundary condition, we use the filter Φ defined as follows:

$$\Phi E(\rho\cos\phi, \rho\sin\phi) = \begin{cases} E(\rho\cos\phi, \rho\sin\phi) & \rho < R \\ -E((2R-\rho)\cos\phi,\ (2R-\rho)\sin\phi)(2R-\rho/R) & R < \rho \leq 2R \\ 0 & \rho \geq 2R \end{cases}. \quad (16)$$

After such filtration, owing to the abrupt change of sign at $\rho = R$, the field again has strong high Fourier components. So we calculate the Fourier transform, truncate it again, and repeat this procedure many times; in practice 10 times were enough to get convergence, and we have a field $\tilde{E} = (\mathcal{F}^\dagger\mathcal{T}\mathcal{F}\Phi)^{10}\mathcal{F}^\dagger \times (\delta\text{-correlated noise})$, where $\mathcal{F}$ is the Fourier operator and a dagger indicates the Hermitian conjugation. Then we construct the normalized field

$$E = \tilde{E}\sqrt{W_0}/\left[\int_{x_1^2+x_2^2<R^2} |\tilde{E}(\mathbf{x}, 0)|^2 \mathrm{d}^2x\right]^{1/2}.$$

The field constructed by filter (16) outside the fiber can be interpreted as the approximate image of the field in the cladding, created by the reflecting surface of the cladding. Figure 2(a) shows an example of the initial distribution of the field constructed in this way. White regions correspond to small values of $|E(x, 0)|$; dark regions represent high values of this modulus. The dashed circles of radii $r = 20M/k$ and $R = 80M/k$ indicate the surface of the core and the surface of cladding. The field has not been affected by the core, but the cladding is clearly seen as a white circle. The image of the distribution reconstructed with the filter Φ is also shown. It is similar to the reflection image of the field, reflected from the walls of the cladding, observed from the interior of the fiber. This field was generated at $p_0 = 0.5k/M$.

First, we considered the propagation of light in the fiber without a core: $\nu = 0$, $\gamma = 0$. Using the operators Φ, we construct the operator that represents one step of propagation: $E(x, z + \zeta) \approx fE(x, z)$, where $f = \Phi\mathcal{F}^\dagger\mathcal{P}\mathcal{F}$ and $\mathcal{P}E_p = E_p\exp[-ip^2/(2k_0)\zeta]$. Before we deal with random fields like those shown in Fig. 2, we examine the propagation of various Bessel modes, comparing the simulation to the exact solution $\Psi_{m,n}\exp[-iq_{m,n}/(2kR^2)z]$. For various modes, the procedure works well at $kq_{m,j}^2/(2kR^2)\zeta < 1$ and begins to fail at $kq_{m,j}^2/(2kR^2)\zeta > 1$. This sets a reasonable limit for the step ζ: it should not be greater than the diffraction length of the field.

For the random field [Fig. 2(a)] and a fiber with an absorbing core, we simulated the linear propagation for a distance $z = 20{,}000M^2/k$ at $\nu_0 = 0.001/M^2$. The final field is shown in Fig. 2(b); the modes with small angular numbers are absorbed, while the whispering gallery modes remain; we see a white spot at the core.

To switch on nonlinearity, we change f to

$$f = \Phi\mathcal{N}\mathcal{F}^\dagger\mathcal{P}\mathcal{F}, \quad (17)$$

where

$$\mathcal{N}E(x) = E(x)\exp[i\nu\zeta + i\gamma|E(x)|^2\zeta]. \quad (18)$$

We repeat the same simulation at $\gamma W_0/k = 70$; the resulting field is shown in Fig. 2(c). The field after propagation for the same distance still has a significant amplitude at the center; the pump continues to deliver its energy into the core.

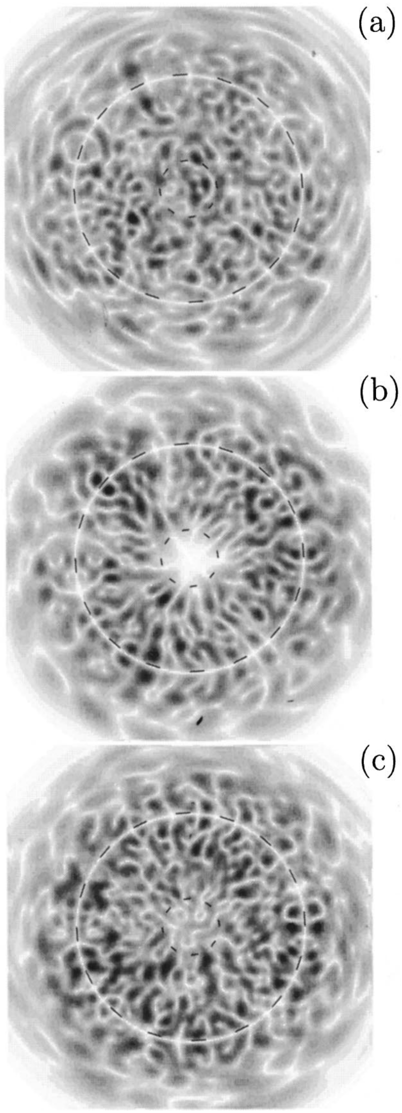

Fig. 2. Distribution of the field amplitude and its image: (a) initial field; (b) after propagation in the linear fiber, $kz = 20000M^2$, $\gamma = 0$; (c) after propagation in the nonlinear fiber, ($\gamma W_0/k = 70$). $p_0 R = 40$, $kR/M = 80$, $kr/M = 20$, $\nu_0 M^2 = 0.001i$.

The propagation of the random initial field was simulated for various values of γ and r, various grids, and various values of the step ζ. Typical examples of the dependence of the efficiency of absorption of the pump in the core are plotted in Fig. 3.

The case in Fig. 3(a) corresponds to $r = 20M/k$, $R = 80M/k$, $p_0 = 0.5k/M$, $\nu_0 = 0.001k/M$. The case in Fig. 3(b) corresponds to $r = 10M/k$, $R = 80M/k$, $p_0 = 0.5k/M$, $\nu_0 = 0.002k/M$. (For simplicity, one can set $M = 1$.)

Curves 5 correspond to the linear case, $\gamma = 0$. Curves 6 represent the approximation Eqs. (8) and (9).

Curves 3 correspond to the simulations with $\gamma W_0/k = -70$ (the case of self-defocusing nonlinearity). Curves 2 (vertical bars) represent the case of $\gamma W_0/k = 70$. The upper end of each bar is evaluated as $(W_0 - W)/W_0$, and the lower end of each bar is calculated by integration of the product of the absorption rate and intensity. Thus the vertical size of the bars approximates the relative error of the numerical solution. Curves 4 represent the asymptotic approximation from Eqs. (8) and (9). Note that, from Eq. (7), the constant of intermodal exchange G depends on the square of γ; thus this approximation detects no difference between the self-focusing and self-defocusing cases. Thus curves 4 should be compared with both curves 3 and 2.

Curves 1 correspond to the case of ideal mixing of the field in the fiber, when the absorbed part of the power at each step is determined by the relation of the cross-section areas of the core and the cladding.

For the simulations above, a 1024×1024 grid was used, with the transverse coordinate step $\mathrm{d}x = 0.25M/k$, the longitudinal coordinate step $\zeta = M^2/k$, and parameter $p_0 = 0.5k/M$. (To be within our paraxial approximation, parameter M should be greater than unity.)

It is typical that the self-defocusing nonlinearity has an effect that is a little smaller than that of self-focusing for

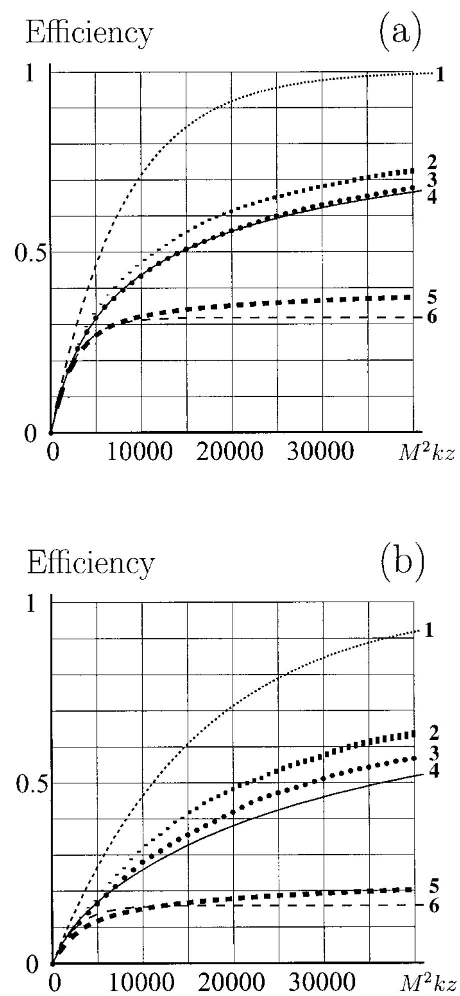

Fig. 3. Efficiency of pump use versus length of propagation. Curves 1 correspond to the case of ideal mode mixing. Curves 2, $\gamma W_0/k = 70$; curves 3, $\gamma W_0/k = -70$; curves 5, linear case ($\gamma = 0$). Curves 6 and 4 represent the geometrical optics approximation as a solution of Eqs. (8) and (9). The grid size is 1024×1024, $\mathrm{Re}(\nu_0) = 0$, $\mathrm{d}x = 0.25M/k$, $p_0 = 0.5k/M$, and $R = 80M/k$. (a) $r/R = 1/4$, $\mathrm{Im}(\nu_0)M/k = 0.001$; (b) $r/R = 1/8$, $\mathrm{Im}(\nu_0)M/k = 0.002$.

the same value of $|\gamma|$. It should be noted that even the detailed kinetic equation for random waves[16] detects no difference between self-focusing and self-defocusing cases. Of course, the physical picture in these two cases is different. In the self-focusing case the increase in nonlinearity is limited by the formation of filaments. In the above simulations the appearance of a filament was observed in numerical experiments at $\gamma W_0/k = 100$. The applicability of the initial equations becomes doubtful in the presence of filaments; thus, here we present results for $\gamma W_0/k = -70, 0, 70$.

The asymptotic formula of Sections 1 and 2 does not take into account the refractive-index step in the core. Simulations with various values of $\mathrm{Re}(\nu_0)$ show that the efficiency's dependence on this step is small. At $|\mathrm{Re}(\nu_0)| < 0.001M^{-2}$, simulations showed that the difference in the efficiency is less than 1%.

We see that nonlinearity can give a significant improvement in the efficiency of pumping a double-clad fiber amplifier. This follows from the speckle-mode consideration of Section 3, as well as from the direct numerical simulation.

Numerical simulations confirm the asymptotic results of Section 3. At appropriate values of the input pump power the efficiency increases from 40% to 70% owing to the nonlinearity for $r/R = 0.25$ and from 20% to 60% for $r/R = 0.125$.

The good agreement of the results of the simulations with the predictions of the speckle-mode approximation demonstrates the applicability of this model in the analysis of double-clad devices. Similar models should also simplify the consideration of fibers with broken symmetry.

The method of approximate images does not use the symmetry of the fiber. So we expect the same operator f, Eq. (17), for a single step of the simulation to work well for other convex claddings, defined with appropriate modification of Eq. (16).

5. ROLE OF THERMAL NONLINEARITY

Here we make a qualitative estimation of the role of thermal nonlinearity in the intermodal exchange. While thermal effects are cumulative, we need to take into account the time dependence of the pump intensity I. Then the equation for the thermally induced variation ν of the refractive index can be written as

$$\dot{\nu} = \kappa \nabla^2 \nu + \mathcal{A} I(\mathbf{x}, t), \tag{19}$$

where a dot indicates the time derivative and ∇ differentiates with respect to coordinates $\mathbf{x}$. In the paraxial approximation all dependences of the third coordinate are slow in comparison with the dependence on the transverse coordinates; so we treat $\mathbf{x}$ as a two-vector.

Constants κ and $\mathcal{A}$ can be expressed in terms of the parameters of the cladding:

$$\kappa = \frac{K}{\rho C}, \qquad \mathcal{A} = \frac{\alpha}{C\rho}\frac{\mathrm{d}n}{\mathrm{d}T},$$

where K is the thermal conductivity, ρ the mass density, C the specific heat capacity, α the absorption decrement, n_0 the background refractive index, and $\mathrm{d}n/\mathrm{d}T$ the thermal sensitivity of the index. For fused silica, and at a pump wavelength of 1 μm, typical values are[17] $K = 1.38\,\mathrm{W/(m\,deg)}$, $C = 0.714\,\mathrm{J/(g\,deg)}$, $\rho = 2.2\,\mathrm{g/cm^3}$, $\alpha = 9 \times 10^{-4}\,\mathrm{cm^{-1}}$, $n_0 = 1.45$, and $\mathrm{d}n/\mathrm{d}T = 9.7 \times 10^{-6}\,\mathrm{deg^{-1}}$.

Assuming periodicity with a large enough scale, we use the Fourier series

$$\nu = \nu(\mathbf{x}, t) = \sum_{\mathbf{q}} \exp(i\mathbf{q}\cdot\mathbf{x})\nu_{\mathbf{q}}(t),$$

$$I = I(\mathbf{x}, t) = \sum_{\mathbf{q}} \exp(i\mathbf{q}\cdot\mathbf{x}) I_{\mathbf{q}}(t). \tag{20}$$

This gives the differential equations for the components $\dot{\nu}_{\mathbf{q}}(t) = -\kappa \mathbf{q}^2 \nu_{\mathbf{q}} + a I_{\mathbf{q}}(t)$; their solution is $\nu_{\mathbf{q}} = \mathcal{A}\int_{-\infty}^{t} \mathrm{d}t_1 I_{\mathbf{q}}(t_1)\exp[-\kappa\mathbf{q}^2(t - t_1)]$. The mean square of the $\mathbf{q}$th component is

$$\langle \nu_{\mathbf{q}}^2 \rangle = \mathcal{A}^2 \int_{-\infty}^{t} \mathrm{d}t_1 \int_{-\infty}^{t} \mathrm{d}t_2 \langle I_{\mathbf{q}}(t_1) I_{\mathbf{q}}(t_2)\rangle \times \exp[-\kappa\mathbf{q}^2(t - t_1) - \kappa\mathbf{q}^2(t - t_2)]. \tag{21}$$

We exclude the case $\mathbf{q} = 0$ because such components do not contribute to the scattering of light and the redistribution of power among modes.

Assume that the mean value on the right-hand side depends only on the difference $t_1 - t_2$; let $\langle I_{\mathbf{q}}(t_1) I_{\mathbf{q}}(t_2)\rangle = J(t_1 - t_2)$. Then, for $\mathbf{q} \neq 0$, we assume a relatively short coherence time in comparison with the relaxation time $\mathcal{T} = 1/(\mathbf{q}^2\kappa)$. (This corresponds to an incoherent pump.) Then we get the estimate

$$\langle \nu_{\mathbf{q}}^2 \rangle \approx \mathcal{A}^2 \int_{-\infty}^{t} \mathrm{d}s \int \mathrm{d}\sigma J_q(\sigma)\exp(-2\kappa\mathbf{q}^2 s) \approx \frac{\mathcal{A}^2\tau}{2\kappa\mathbf{q}^2}\langle I_{\mathbf{q}}^2\rangle,$$

where τ is some typical scale of decay of the correlation function J. Estimating δn as the square root of sum of $\nu_{\mathbf{q}}^2$ with respect to some reasonable region of values of $|\mathbf{q}|$ around some reasonable effective q_{eff}, we get $\delta n \approx (n_2)_{\mathrm{eff}} I_0$, where I_0 is the typical intensity and

$$(n_2)_{\mathrm{eff}} \approx \mathcal{A}\left(\frac{\tau}{2\kappa q_{\mathrm{eff}}^2}\right)^{1/2} = \frac{\alpha}{q_{\mathrm{eff}}}\frac{\mathrm{d}n}{\mathrm{d}T}\left(\frac{\tau}{2K\rho C}\right)^{1/2} \tag{22}$$

is the estimate of the effective nonlinear constant. Owing to the nonlocal character of thermal processes, this constant depends on the effective wave number. Estimating this wave number as $q_{\mathrm{eff}} = 10^3\,\mathrm{cm^{-1}}$ (still greater than the value of $1/R$ from the estimate of Section 3), and assuming the time of correlation of intensity of field $\tau = 10^{-5}\,\mathrm{s}$, we get the estimate $(n_2)_{\mathrm{eff}} \approx 10^{-13}\,\mathrm{cm^2/W}$, which is 3 orders of magnitude greater than the constant for the Kerr nonlinearity in silica fibers discussed above. We have no certain data about the thermal nonlinear constant for optical polymers, but we expect that for polymer cladding the thermal effect is even stronger.

The effect depends on the time τ, which characterizes fluctuations of the pump intensity. (Speckle structure changes at the rate $1/\tau$). For a quasi-monochromatic pump with an almost static speckle pattern, τ is large, and the thermal effect should be dominant among natural mechanisms mixing modes.

Note that the effect of electrostriction may cause some resonant backscattering.[10] The pump backscattered by even a small amount should cause the partial synchronization of pump lasers. Such synchronization may cause long-living components $I_{\mathbf{q}}$. (Then the approximation $\mathcal{T} \gg \tau$ used above to evaluate the integral with respect to ds would not be valid.) The long-living intensity components would cause inhomogeneities even stronger than those estimated above.

6. RESULTS AND CONCLUSION

We suggest a simple formula to estimate the efficiency of the nonlinear coupling of the pump into the core in a double-clad fiber [Eqs. (11) and (12)]. This formula is the limiting case of the asymptotic equations (7)–(9) deduced on the basis of the speckle-mode approximation and geometrical optics.

We describe an original method of approximate images used to simulate the propagation of an optical field in a waveguide with a curvilinear surface, employing a rectangular grid and the fast Fourier transform; the elementary step of propagation is expressed with Eq. (17). We apply this method to the simulation of a double-clad fiber with circular symmetry, and in Fig. 3 we compare the results with solutions of the asymptotic equations. Good agreement is established.

Any fluctuations of the index of refraction may improve the efficiency of the noncoherent pump in any double-clad fiber. Equation (14) gives a quantitative estimate of role of this effect in fibers with circular symmetry. Internal inhomogeneities of the cladding may cause this effect, but such fluctuations are difficult to measure directly to test this conclusion experimentally. We suggest the use of the Kerr nonlinearity. In that case fluctuations are easy to evaluate, and our results allow a direct experimental test with a pulsed pump. For a continuous pump in silica fibers, the Kerr nonlinearity is too small. In the case of a polymer cladding we expect that the nonlinearity causes a significant effect even for the continuous pump used in commercial double-clad fiber amplifiers. The method of approximate images allows generalization to the case of cladding with broken circular symmetry.[18]

The thermal nonlinearity also should mix the modes of the double-clad fiber, improving the coupling of power of the pump into the core. This effect is sensitive to the time of correlation of the intensity of the pump.

ACKNOWLEDGMENTS

The authors are grateful to Robert M. Indik and Miroslav Kolesik for help and discussions. This work was supported by U.S. Air Force Office of Scientific Research grants F49620-00-1-0002, F49620-00-1-0190 and, in part, by National Science Foundation Grant Opportunities for Academic Liaison with Industry grant DMS 9811466.

E-mail addresses are, for D. Kouznetsov, dima@acms.arizona.edu; for J. V. Moloney, jml@acms.arizona.edu; for E. M. Wright, ewan.wright@optics.Arizona.EDU.

REFERENCES

1. R. Oron and A. A. Hardy, "Rayleigh backscattering and amplified spontaneous emission in high-power yttrium-doped fiber amplifiers," J. Opt. Soc. Am. B **16**, 695–701 (1999).
2. D. J. DiGiovanni and M. H. Muendel, "High-power fiber lasers and amplifiers," Opt. Photon. News **10**, 26–30 (1999).
3. V. Dominic, S. MacCormac, R. Waarts, S. Bicknese, R. Dohle, E. Wolak, P. S. Yeh and E. Zukert, "110 W fiber laser," Electron. Lett. **35**, 1158–1160 (1999).
4. N. S. Kim, T. Hamada, M. Prabhu, C. Li, J. Sing, K. Ueda, A. Liu, and H. J. Kong, "Numerical analysis and experimental results of output performance for Nd-doped double-clad fiber lasers," Opt. Commun. **180**, 329–337 (2000).
5. A. Liu and K. Ueda, "The absorption characteristics of circular, offset, and rectangular double-clad fibers," Opt. Commun. **132**, 511–618 (1996).
6. S. Bedö, W. Lüthy, and H. P. Weber, "The effective absorption coefficient in double-clad fibers," Opt. Commun. **99**, 331–335 (1993).
7. D. Kuznetsov, "Transformation of transversal structure of monochromatic light in nonlinear media," in *Optics and Lasers*, V. A. Shcheglov, ed. (Nova Science, New York, 1996).
8. D. Yu. Kuznetsov, "Interaction between a spatially modulated wave with a complex structure and a plane wave in a medium with nonlinear refraction," Sov. J. Quantum Electron. **16**, 408–420 (1986).
9. B. Ya. Zeldovich and T. I. Yakovleva, "Distortions of a fine-structure wave pattern due to self-focusing nonlinearity," Sov. J. Quantum Electron. **10**, 757–759 (1980).
10. A. Newell and J. Moloney, *Nonlinear Optics* (Addison-Wesley, New York, 1992).
11. M. Yamashita, K. Torizuka, and T. Uemiya, "Efficient compression of femtosecond laser pulses using nonlinear optical fibers," in *Nonlinear Optics. Fundamental, Materials and Devices*, S. Miyata, ed. (Elsevier Science, Amsterdam, 1992).
12. N. Tanio and Y. Koike, "What is the most transparent polymer?" Polymer J. **32**, 43–50 (2000).
13. G. I. Stegeman, C. T. Seaton, W. M. Heterington, A. D. Boardman, and P. Egan, "Nonlinear guided waves," in *Nonlinear Optics: Materials and Devices*, C. Flytzanis and J. Louder, eds. (Springer-Verlag, Berlin, 1985).
14. Y. Ogawa and K. Ootani, "Synthesis of nonlinear optical side-chain polymers containing the carbozolyldinitrophenyl-hydrazine moiety by polymer reaction," Polymer J. **31**, 55–60 (1999).
15. M. Sylla, D. Manaila-Maximean, A. M. Albu, and J. Delaunow, "Synthesis, characterization and nonlinear optical properties of polymers based on colored monomers," Polymer **41**, 3507–3511 (2000).
16. V. E. Zakharov, V. S. Lvov, and G. Falkovich, *Kolmogorov Spectra of Turbulence. I. Wave Turbulence* (Springer-Verlag, New York, 1992).
17. A. Feldman, D. Horovitz, and R. M. Waxler, "Mechanisms for self-focusing in optical glasses," IEEE J. Quantum Electron. **QE-9**, 1054–1061 (1973).
18. D. Kouznetsov and J. V. Moloney, "Efficiency of pump absorption in double-clad fiber amplifiers. II. Broken circular symmetry," submitted to J. Opt. Soc. Am. B.